

## PUBLISHED VERSION

Ruan, Yinlan; Foo, H.; Warren-Smith, Stephen Christopher; Hoffmann, Peter; Moore, Roger Charles; Ebendorff-Heidepriem, Heike; Monro, Tanya Mary

[Antibody immobilization within glass microstructured fibers: A route to sensitive and selective biosensors](#), Optics Express, 2008; 16(22):18514-18523.

© 2008 Optical Society of America

### PERMISSIONS

[http://www.opticsinfobase.org/submit/review/copyright\\_permissions.cfm#posting](http://www.opticsinfobase.org/submit/review/copyright_permissions.cfm#posting)

This paper was published in Optics Express and is made available as an electronic reprint with the permission of OSA. The paper can be found at the following URL on the OSA website

<http://www.opticsinfobase.org/oe/abstract.cfm?uri=oe-16-22-18514>

Systematic or multiple reproduction or distribution to multiple locations via electronic or other means is prohibited and is subject to penalties under law.

Transfer of copyright does not prevent an author from subsequently reproducing his or her article. OSA's Copyright Transfer Agreement gives authors the right to publish the article or chapter in a compilation of the author's own works or reproduce the article for teaching purposes on a short-term basis. **The author may also publish the article on his or her own noncommercial web page ("noncommercial" pages are defined here as those not charging for admission to the site or for downloading of material while on the site).** In addition, we allow authors to post their manuscripts on the Cornell University Library's [arXiv](#) site prior to submission to OSA's journals.

18<sup>th</sup> September 2013

<http://hdl.handle.net/2440/47928>

# Antibody immobilization within glass microstructured fibers: a route to sensitive and selective biosensors

Yinlan Ruan<sup>1</sup>, Tze Cheung Foo<sup>1</sup>, Stephen Warren-Smith<sup>1</sup>, Peter Hoffmann<sup>2</sup>, Roger C. Moore<sup>1</sup>, Heike Ebendorff-Heidepriem<sup>1</sup>, Tanya M. Monro<sup>1</sup>

<sup>1</sup>Centre of Expertise in Photonics, School of Chemistry & Physics

<sup>2</sup>Adelaide Proteomics Centre, School of Molecular & Biomedical Science

University of Adelaide, Adelaide, SA 5005, Australia

\*Corresponding author: [yinlan.ruan@adelaide.edu.au](mailto:yinlan.ruan@adelaide.edu.au)

**Abstract:** Glass microstructured optical fibers have been rendered biologically active for the first time via the immobilization of antibodies within the holes in the fiber cross-section. This has been done by introducing coating layers to the internal surfaces of soft glass fibers. The detection of proteins that bind to these antibodies has been demonstrated experimentally within this system via the use of fluorescence labeling. The approach combines the sensitivity resulting from the long interaction lengths of filled fibers with the selectivity provided by the use of antibodies.

©2008 Optical Society of America

**OCIS codes:** (060.2370) Fiber optics sensors; (170.6280) Spectroscopy fluorescence and luminescence; (300.1030) Absorption; (300.2140) Emission.

---

## References and links

1. J. B. Jensen, P. E. Hoiby, G. Emilianov, O. Bang, L. H. Pedersen, and A. Bjarklev, "Selective detection of antibodies in microstructured polymer optical fibers," *Opt. Express* **13**, 5883-5889 (2005), <http://www.opticsinfobase.org/oe/abstract.cfm?URI=oe-13-15-5883>.
2. L. Rindorf, P. E. Hoiby, J. B. Jensen, L. H. Pedersen, O. Bang, and O. Geschke, "Towards biochips using microstructured optical fiber sensors," *Anal. Bioanal. Chem.* **385**, 1370-5 (2006).
3. C. M. B. Cordeiro, M. A. R. Franco, G. Chesini, E. C. S. Barretto, R. Lwin, C.H.B. Cruz, and M.C.J. Large, "Microstructured-core optical fibre for evanescent sensing applications," *Opt. Express* **14**, 13056-13066 (2006), <http://www.opticsinfobase.org/oe/abstract.cfm?URI=oe-14-26-13056>.
4. Y. Zhu, H. Du, and R. Bise, "Design of solid-core microstructured optical fiber with steering-wheel air cladding for optimal evanescent-field sensing," *Opt. Express* **14**, 3541-3546 (2006), <http://www.opticsinfobase.org/oe/abstract.cfm?URI=oe-14-8-3541>.
5. T. Ritari, J. Tuominen, H. Ludvigsen, J. C. Petersen, T. Sorensen, T. P. Hansen, and H. R. Simonsen, "Gas sensing using air-guiding photonic bandgap fibers," *Opt. Express* **12**, 4080-4087 (2004), <http://www.opticsinfobase.org/oe/abstract.cfm?URI=oe-12-17-4080>.
6. Y. Ruan, E. P. Schartner, H. Ebendorff-Heidepriem, P. Hoffmann, and T. M. Monro, "Detection of quantum-dot labelled proteins using soft glass microstructured optical fibers," *Opt. Express* **15**, 17819-17826 (2007), <http://www.opticsinfobase.org/oe/abstract.cfm?URI=oe-15-26-17819>.
7. L. Rindorf, J. B. Jensen, M. Dufva, L. H. Pedersen, P. E. Hoiby, and O. Bang, "Photonic crystal fiber long-period gratings for biochemical sensing," *Opt. Express* **14**, 8224-8231 (2006), <http://www.opticsinfobase.org/oe/abstract.cfm?URI=oe-14-18-8224>.
8. J. Cheng, C. Wei, K. Hsu, and T. Young, "Direct-write laser micromachining and universal surface modification of PMMA for device development," *Sens. Actuators B*, **99**, 186-196 (2003).
9. G. Emilianov, J. B. Jensen, and O. Bang, "Localized biosensing with Topas microstructured polymer optical fiber," *Opt. Lett.* **32**, 460-462 (2007).
10. F. M. Cox, R. Lwin, M. C. J. Large, and C. M. B. Cordeiro, "Opening up optical fibres," *Opt. Express* **15**, 11843-11848 (2007), <http://www.opticsinfobase.org/oe/abstract.cfm?URI=oe-15-19-11843>.
11. C. M. B. Cordeiro, C. J. S. de Matos, E. M. dos Santos, A. Bozolan, J. S. K. Ong, T. Facincani, G. Chesini, A. R. Vaz, and C. H. B. Cruz, "Towards practical liquid and gas sensing with photonic crystal fibers: side access to the fibre microstructured and single-mode liquid-core fibre," *Meas. Sci. Technol.* **18**, 3075-3081 (2007).

12. P. D. Sawant, G. S. Watson, S. Myhra, and D. V. Nicolau, "Hierarchy of DNA immobilization and hybridization on poly-L-lysine using an atomic force microscopy study," *J. Nanosci. Nanotechnol.* **5**, 951–957 (2005).
13. J. Debs, H. Ebendorff-Heidepriem, J. Quinton, and T. M. Monro, "A Fundamental study into the surface functionalisation of soft glass microstructured optical fibres via silane coupling agents," accepted for publication, *J. Lightwave Technol.* (2008).
14. S. Gosh, A. R. Bhagwat, C. K. Renshaw, S. Goh, A. L. Gaeta, and B. J. Kirby "Low-light-level optical interactions with rubidium vapor in a photonic band-gap fiber," *Phys. Rev. Lett.* **97**, 023603 (2006).
15. H. Ebendorff-Heidepriem and T. M. Monro, "Extrusion of complex preforms for microstructured optical fibers," *Opt. Express* **15**, 15086-15092 (2007), <http://www.opticsinfobase.org/oe/abstract.cfm?URI=oe-15-23-15086>.
16. H. Ebendorff-Heidepriem, S. C. Warren-Smith, and T. M. Monro, "Suspended nanowires: fabrication, design, and characterization of fibers with nanoscale cores," submitted to *Nature Photonics*.
17. S. Afshar V. S. C. Warren-Smith, and T. M. Monro, "Enhancement of fluorescence-based sensing using microstructured optical fibers," *Opt. Express* **15**, 17891-17901 (2007), <http://www.opticsinfobase.org/oe/abstract.cfm?URI=oe-15-26-17891>.
18. S. K. Bhatia, L. C. Shriver-Lake, K. J. Prior, J. H. Georger, J. M. Calvert, R. Bredehorst, and F. S. Ligler, "Use of thiol-terminal silanes and heterobifunctional crosslinkers for immobilization of antibodies on silica surfaces," *Anal. BioChem.* **178**, 408-413 (1989).
19. T. M. Monro, Y. Ruan, H. Ebendorff-Heidepriem, H. Foo, P. Hoffmann, and R. C. Moore, "Antibody immobilization with glass microstructured fibers: a route to sensitive and selective biosensor," *Proc. Internat. Soc. Opt. Engin. (SPIE)* **17**, 70046Q-1-4 (2008).
20. S. C. Warren-Smith, S. Afshar, and T. M. Monro, "Highly-efficient fluorescence sensing using microstructured optical fibres; side access and thin-layer configurations," *Proc. Internat. Soc. Opt. Engin. (SPIE)* **17**, 70041X-1-4 (2008).
21. <http://www.invitrogen.com/site/us/en/home/brands/Product-Brand/Qdot/Technology-Overview.html>.
22. <http://probes.invitrogen.com/products/qdot/>.
23. J. R. Crowther, *ELISA: Theory and Practice* (Humana, 1995).
24. S. Afshar, Y. Ruan, and T. M. Monro, "Enhanced fluorescence sensing using microstructured optical fibers: a comparison of forward and backward collection modes," *Opt. Lett.* **33**, 1743-1745 (2008).

## 1. Introduction

Microstructured optical fibers (MOFs) have the potential to provide improved performance relative to more traditional spectroscopic and fluorescence-based fiber sensors [1-6]. The manipulation of the geometry of the fiber cross-section can increase the fraction of the guided light that is available to interact with the environment to be sensed. The application of MOF-based sensors for the detection of biomolecules is of particular interest, and previous work includes the detection of antibodies in solution [1], the detection of proteins in solution down to the 1 nM level [6], and the detection of the thickness of DNA layers [7]. The first two examples rely on the use of fluorescently labeled biomolecules, with the fluorescence signal being collected via excitation of the guided mode of the fiber.

The development of effective MOF-based biosensors requires: 1) a sensitive detection mechanism capable of measuring low-levels of biomolecules and 2) a means of selectively identifying specific biomolecules of interest. The first requirement can be realized by taking advantage of the long interaction lengths offered by the interaction between a guided mode in a fiber and the material of interest. It has been possible to detect proteins at the 1 nM level using soft glass MOFs [6].

The introduction of selectivity to an MOF-based sensor requires the functionalization of the otherwise inert fiber to allow its response to a biological species to be determined via optical measurements. In principle, this can either be done during the fiber fabrication process or via post-processing of the fiber.

One advantage of using polymer MOFs is that the surface can be chemically modified to allow biomolecules to be attached directly [1, 8, 9]. The low glass transition temperature (e.g. ~90 °C for PMMA) makes polymer fibers impractical for use in high temperature environments or for high power light transmission. Although glass MOFs do not allow direct functionalization, their potential benefits for biosensing are great, since they offer access to particular spectral regions such as the UV-Vis (via high purity silica glass) and the mid-IR (via soft glasses such as tellurite, fluorides, and chalcogenides). Compared to polymer MOFs,

glass MOFs have other advantages including lower loss, the potential for higher damage thresholds because of their higher glass transition temperatures, better cleaving, and easier integration with conventional fiber technologies. This motivates the investigation of approaches for functionalizing glass-air boundaries within glass MOFs.

For glass fibers, which have relatively high processing and fabrication temperatures, the most promising approach for incorporating biological functionality within the fiber is to deposit surface layers after the fiber has been drawn. This post-processing can be done from the end of the fiber or via side access holes. Side access holes can be produced by techniques such as drilling at the preform stage, or ion beam milling at the fiber stage [10,11]. While side-access is attractive for distributed detection schemes, only limited lengths have been fabricated in glass fibres [11]. For the work presented here, we choose to explore the approach of functionalizing fibers from the fiber ends, which requires the development of techniques for depositing coatings on the internal surfaces of the holes within the cross-section and along the length of the fiber.

Recently, the internal surfaces of silica MOFs have been coated with strands of DNA [7]. This approach uses poly-L-lysine to immobilize negatively charged molecules such as DNA to a solid support. Poly-L-lysine has positively charged amino-groups that can bind to the negatively charged silica surface through an ionic binding [12]. An alternate approach is based on coating the internal surfaces of soft glass MOFs with nm-scale silane layers [13]. A similar process has been used to coat the core of a photonic bandgap fiber with a silane coating [14].

Here we demonstrate that it is possible to extend this technique to allow the immobilization of antibodies inside soft glass MOFs. Soft glasses have lower glass softening points than silica, enabling preform and jacket tube fabrication via extrusion through complex stainless steel dies [15]. The extrusion technique allows a large flexibility in the preform and jacket tube geometries that can be achieved. This, in turn, has recently enabled the fabrication of fibers with nanoscale core sizes as small as 400 nm diameter (without requiring a postprocessing tapering step), which is of great advantage for sensing applications [16]. Furthermore, for nanoscale core sizes, the higher refractive indices of soft glasses compared with silica enables higher sensitivity due to enhanced fluorescence capture fraction [17].

The immobilization of antibodies inside soft glass MOFs is based on adapting the established procedure used for the immobilization of antibodies onto glass slides [18] to the internal holes within an MOF, and here we implement this procedure in non-silica glass fibers for the first time. Proof of concept of this approach was demonstrated in Ref. [19]. Here we present a detailed description of the experimental demonstration of the selective detection of immobilized proteins within a glass fiber. In Section 2, the immobilization processes and experimental results on bulk glasses are introduced. The way in which these processes can be applied to soft F2 glass MOF for biosensing is then described in Section 3.

## **2. Antibody immobilization on glass**

To detect specific proteins, it is necessary to immobilize antibodies onto the glass surface that forms the fiber core in order to facilitate the selective binding of antigens to antibodies to occur in a region where the overlap with the guided mode of the fiber is strong. However, as mentioned above, antibodies cannot be attached directly to a glass surface. Bhatia et al. [18] immobilized antibodies onto glass slides by first introducing silane and crosslinked layers. In brief, first a silane layer is attached to the glass surface, followed by attachment of a so-called crosslinker onto the silane layer. Finally, the antibodies are attached to the crosslinker [18]. A solution containing a range of antigens that may be labeled with different dyes can then be introduced into the holes of the fiber by dipping the end of the fiber into the solution and allowing it to fill under capillary action. The antigens that correspond to the immobilized antibodies will bind to them, and any unmatched antigen can be flushed away.

Here we adapt the immobilization procedures described by Bhatia [18] for use in glass films to our fiber/glass geometry. This process begins with the cleaning of the glass surface to remove debris and to create hydroxyl groups. The next step is the silanization of the internal

surfaces (for more detail, see Ref. [13]), and then a cross-linking layer is formed to connect the silane layer to the antibody. The procedures utilize thiol-terminal silanes and heterobifunctional crosslinkers with different reactive groups on each end. One end of the crosslinker is coupled to the silane film and another end forms an amide bond with a terminal amino group on the antibody. The material we choose for silanization is 3-Mercaptopropyltrimethoxysilane [Sigma]. The organic crosslinking agent is N- $\gamma$ -maleimidobutyryloxy succinimide ester (GMBS) [Merck]. Five proteins were chosen for our tests of selective detection, and they are mentioned below as required.

### 2.1 Demonstration of immobilization on glass plates

This immobilization process was first tested on glass plates made from 3 different glass materials: conventional glass slides, F2 and LLF1 glass plates. F2 and LLF1 glasses are commercially available Schott glasses. To obtain a hydrophilic surface for silanization, the glass plates are first cleaned with a mixture of concentrated hydrochloric acid and methanol, and then treated with concentrated sulphuric acid. After cleaning, the oxide surfaces of the glass plates exhibit a relatively low water contact angle (that is, a more hydrophilic surface). After silanization, the contact angle of water with the glass plates is  $52^\circ$ , in agreement with literature [18]. Similar results are obtained for the F2 and LLF1 plates. The silane and crosslinker layers were attached via immersion of the glass plates in the corresponding solutions. To reduce cost, in most of our experiments, a single drop (30  $\mu$ L) of antibody/antigen solution was placed on the glass surface for incubation to achieve protein immobilization or binding.

To determine whether the antibodies were attached to the glasses, we labeled the antibodies with quantum dots, whose fluorescence was detected with a Typhoon imager. The imager is equipped with lasers at 488, 532, and 630 nm, and has filters to block the excitation light and improve the image contrast. We used two different quantum dots, which separately emit light at 800 nm (Qdot800) and at 705 nm (Qdot705).

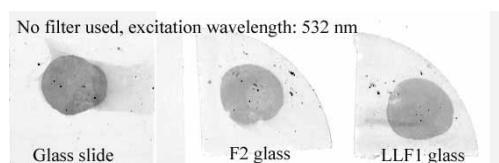


Fig. 1. Images of the glass samples with immobilized Q800-labeled antibodies.

The first antibody sample used here is Qdot800 goat F(ab')<sub>2</sub> anti-mouse IgG conjugate. The maximum wavelength of the filters within the imager is 670 nm (30 nm bandwidth), which will block 800 nm emission from the Qdots used for antibody labeling [6]. Thus no filter was used for fluorescence measurement of the samples with Qdot800 labeled antibodies. A 532 nm laser was chosen as an excitation source. This selection was made as a result of a trade-off between the loss of the glass at the pump wavelength, the source availability, and the pump absorption. Figure 1 shows the images of the three glass plates with each treated via application of a 100 nM 30  $\mu$ L antibody solution drop. The drop was firstly allowed to remain on the glass surface for one hour before the plate was rinsed using deionized water. The area the antibody drop covered appears dark in color and indicates strong fluorescence from Qdot800, demonstrating that the antibody has attached to the glass surfaces via silane and cross-linked layers. The contrast of the fluorescence signal between the droplet and the background regions is clear. The signal from the conventional slide is stronger than the other glasses, indicating higher attachment efficiency for the slides compared to the F2 and LLF1 glasses.

To further test the immobilization process, we used an antibody labeled with an alternative quantum dot (Qdot705 goat F(ab')<sub>2</sub> anti-mouse IgG conjugate) with an emission wavelength located at 705 nm. When the image of the glass slide immobilized with this

conjugate was taken together with those of the F2 and LLF1 samples immobilized with the Qdot 800 labeled antibody (Fig. 1) using the 670 nm filter, only the glass slide presents the antibody drop image with the emissions from Qdot800 on the F2 and LLF1 glasses removed by the filter. This confirmed that all the drop images are produced by fluorescence light emitted by the Qdot-labeled antibodies.

To determine the quantity of immobilized antibody, the image of the drop with the same volume (30  $\mu$ L) and concentration of the antibody on the glasses has been taken as a reference. Image analysis software (IMAGEQUANT SOLUTIONS) has been used for signal quantification. Figure 2 shows the image of the drop of 100 nM 30  $\mu$ L Qdot800 goat F(ab')<sub>2</sub> anti-mouse IgG conjugate, which remained on the glass slide when the image was taken. The object and background are defined in Fig. 2 for fluorescence analysis. The total fluorescence of the image is obtained by integrating the signal corresponding to the object and subtracting the background. Table 1 summarizes the ratios of the total fluorescence of the images shown in Fig. 1 relative to that of the standard 100 nM 30  $\mu$ L antibody drop shown in Fig. 2. Based on the concentration of the drop and their image areas, the density of the immobilized antibody can be extracted. As shown in Table 1, the relative immobilization efficiency was found to be: conventional glass slide > LLF1 glass > F2 glass.

In Table 1, our results are also compared with previous results reported in Ref. [18] for glass slides and silica. Since different antibody concentrations were used, we normalized the immobilized antibody surface density,  $S$ , to the concentration of the antibody solution,  $C$ . The thus obtained parameter  $d = S/C$  represents the minimum thickness of a depletion layer at the substrate surface, i.e. it corresponds to a solution layer on the surface, which is completely depleted of antibody molecules since all the antibodies are immobilized onto the glass surface. The thus defined minimum depletion layer thickness allows comparison of immobilization results for different solution concentrations, which shows that our experiments achieve similar immobilization efficiency to that of Ref. [18]. As is shown below, this parameter also allows comparison between a larger solution volume and a solution confined in a small fiber hole.

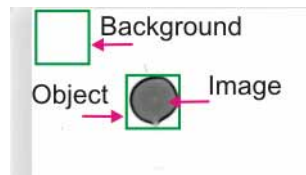


Fig. 2. Fluorescence image of the standard 30  $\mu$ L 100 nM antibody drop on the glass slide. The definition of the object and background for fluorescence analysis is also displayed.

Table 1. Antibody immobilization for different glasses

		antibody concentration C (nM)	fluorescence intensity relative to standard volume	immobilized surface density S (fmol/mm <sup>2</sup> )	depletion layer thickness $d = S/C$ ( $\mu$ m)
Ref. [18]	silica	312		6	19
	glass slide	312		4	13
this work	glass slide	100	0.0186	1.4	14
	LLF1 plate	100	0.0156	1.1	11
	F2 plate	100	0.0136	0.9	9
	F2 MOF	100		max. 0.2	

## 2.2 Quantification of the binding efficiency of the antibody to the antigen

Following the quantification of the density of the immobilized antibodies on the glass surfaces, the next step is to quantify the binding efficiency of the antibodies to the antigens. Two binding experiments were performed. For the first binding experiment, 30  $\mu\text{L}$  100 nM unlabeled antigen (purified mouse IgG) was firstly immobilized on the treated glass slide. Then one 30  $\mu\text{L}$  drop of 100 nM labeled antibody (Qdot800 goat F(ab')<sub>2</sub> anti-mouse IgG conjugate) was put on the surface of the glass slide for one hour, and then was washed away using deionized water. Usually if the antibody treated substrate is incubated in a so-called blocking agent solution, the number of the antigens attached to the crosslinker is negligible [18]. Note that for these preliminary experiments no blocking agents were used. The image of the treated glass slide is shown in Fig. 3(a). The darker area in the center corresponds to the labeled antibody drop, indicating the antibody has been attached to the substrate. The attached antibody density is 0.40 fmol/mm<sup>2</sup> based on its fluorescence intensity relative to the standard in Fig. 2. Since no blocker was used, this antibody density comprises antibodies immobilized to the antigens and adsorbed to the crosslinker. The total density of the antibodies coupled to the substrate relative to the density of immobilized antigens is 44%, smaller than that achieved in Ref. [18] (60%), which resulted from higher concentration (330 nM) antibody/antigen solutions for immobilization and binding. Thus the different binding efficiency is attributed to the use of F2 glass and to the use of lower concentrations (100 nM) for the antibody and antigen solutions in our experiment.

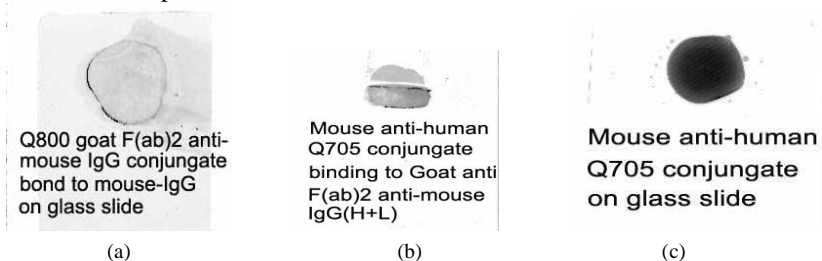


Fig. 3. Binding between antibody and antigen with only one of them labeled: (a) labeled antibody (Qdot800 goat F(ab')<sub>2</sub> anti-mouse IgG conjugate) bond to unlabeled antigen (Purified mouse IgG); (b) antigen (mouse anti-human Qdot705 conjugate) bond to unlabeled antibody (Goat anti-Fab2 anti-Mouse IgG (H+L)); (c) 30  $\mu\text{L}$  100 nM antigen solution (mouse anti-human Qdot705 conjugate) as a reference.

In any practical sensor, it is necessary to use specific antibodies to detect specific antigens within the sample. Thus for the second experiment, we reversed the sequence of the antibody and antigen. The unlabeled antibody (goat anti-Fab2 anti-Mouse IgG (H+L)) was first immobilized onto the treated LLF1 glass slide. A large volume (>130  $\mu\text{l}$ ) was used to allow immobilization to occur across the whole surface. A high concentration (330 nM) was used to increase the density of the immobilized antibody (and of the bound antigen). Indeed, a thick antibody layer was observed after immobilization (with a 100 nM antibody solution, the layer is not evident to the eye). Following a rinse using the buffer solution, a portion of the layer washed away, indicating weak attachment between the thick antibody layer and the crosslinked film. Applying a 30  $\mu\text{L}$  100 nM antigen solution (Qdot705 mouse anti-human conjugate) on the surface of the remained thick film for one hour and then washing the antigen solution away, the image of the bound antigen is shown in Fig. 3(b). Figure 3(c) shows the image of the antigen solution drop with the same concentration/volume as that used in Fig. 3(b). Through comparing the fluorescence signals of Fig. 3(b) and 3(c), and calculated antigen number included in the antigen drop in the Fig. 3(c), the calculated density of the attached antigen in Fig. 3(b) is 2.5 fmol/mm<sup>2</sup>. This corresponds to 68% total density of immobilized antigen relative to the density of immobilized antibody. As expected, a higher binding density results from a higher density of immobilized antibody. This value is also equivalent to that achieved on the silica substrate in Ref. [18], where no blocker was used as

well. Since no blocker was used, nonspecific binding of antigen or antibody to the crosslinker layer was not prevented. For the silica substrate, Ref. [18] demonstrated that the nonspecific binding represented 38% of the total binding to antigen and crosslinker [18]. The ratio of nonspecific binding to the specific binding is believed to be mainly dependent on respective reactivity of the antigen to the antibody and to the crosslinker. Thus we can conclude that specific antigen binding has been achieved in the LLF1 glass.

### 3. Application to fibers for biosensing

The F2 glass MOFs used in this work have a fiber core that is suspended in air by 3 long fine struts within a robust jacket. An SEM image of one of these fibers is shown in Fig. 4(a). These fibers have been fabricated in-house, and we have very recently achieved core diameters as small 400 nm using this design concept [16]. For the preliminary experimental work described here, MOFs with relatively large core diameter of 1.3  $\mu\text{m}$  and relatively large hole radius of  $\sim 4.3 \mu\text{m}$  were chosen to enable high coupling efficiency and fast filling of the air holes. In order to adapt the immobilization processes developed for bulk glasses to the internal surfaces of optical fibers, we omitted the cleaning step for immobilization within the MOF, since the internal surfaces of the MOF are fire-polished during fabrication and are unlikely to be contaminated. After every step, in order to avoid previous chemicals left within the MOF, a specific solution (buffer or deionized water) was used to flush the MOF. A pump was used to fill and empty the fibers with the required liquids [13]. The time for filling is set to 2 hours and for emptying is 1 hour using our pumping system. Note that in a practical application this can be reduced significantly using higher pressure filling, larger holes, or both. In addition, not all of the fiber needs to be filled in order to make a measurement provided that one is not operating near the detection limit of the system. The protein used for immobilization on the internal hole surfaces of the fiber is 100 nM Qdot800 goat F(ab')<sub>2</sub> anti-mouse IgG conjugate.

After immobilization, the loss of the F2 MOF increased to about 30 dB/m at 532 nm compared to 2 dB/m before processing. The reason for this increased fiber loss is not entirely clear and requires further investigation. Thus only a short fiber could be used for observation of fluorescence. The same setup was used for fluorescence measurement as illustrated in Ref. [6]. The measured fluorescence signals with different output power from the 19.2 cm long F2 MOF with immobilized antibodies is shown in Fig. 4(b). The background fluorescence from the MOF itself has been subtracted in Fig. 4(b). The strong fluorescence clearly indicates that antibodies have become attached to the core surface. Figure 4(c) shows the fluorescence signal of another F2 MOF with 25 cm length from the same fiber draw as that used in Fig. 4(a) but instead filled with a 100 nM antibody solution. Both fibers have the same core size, and the same experimental conditions were used. Note that the loss of the solution filled F2 MOF was only 2 dB/m. Comparing Fig. 4(b) and 4(c), it can be seen that the F2 MOF with immobilized antibody exhibits a fluorescent signal about 10% of that from the MOF filled with solution.

To predict the density of the immobilized antibody on the core surface, and also the potential of the immobilized fiber for sensing, the fluorescence capture within the immobilized MOFs is compared with solution-filled MOFs has been calculated using the models recently developed by our group [17,20]. In order to simplify these calculations, a step-index structure is used for these calculations. For the antibody solution filled fibers, the model assumes that a length of MOF is fully filled with the solution. For the immobilized fibers, a single molecular layer is assumed to be immobilized on the core surface. Thus the distance from the Qdots to the surface of the fiber core is regarded as layer thickness, and is approximately 10 nm according to the data provided by Invitrogen [21]. The extinction coefficient of the Qdots is  $2 \times 10^8 \text{ M}^{-1}\text{m}^{-1}$  [22]. The loss of the solution-filled MOF at the excitation wavelength of 790 nm was measured as 1 dB/m using a standard cut-back measurement. The fluorescence measurements are made at the opposite end of the fiber from which the pump light is launched. The calculated ratio of the captured fluorescence in the immobilized fiber (with a loss of 30 dB/m) to that in the solution-filled MOF is shown in Fig. 5(a). This quantity is described as the ratio of the fluorescence capture fraction (FCF) in Fig.



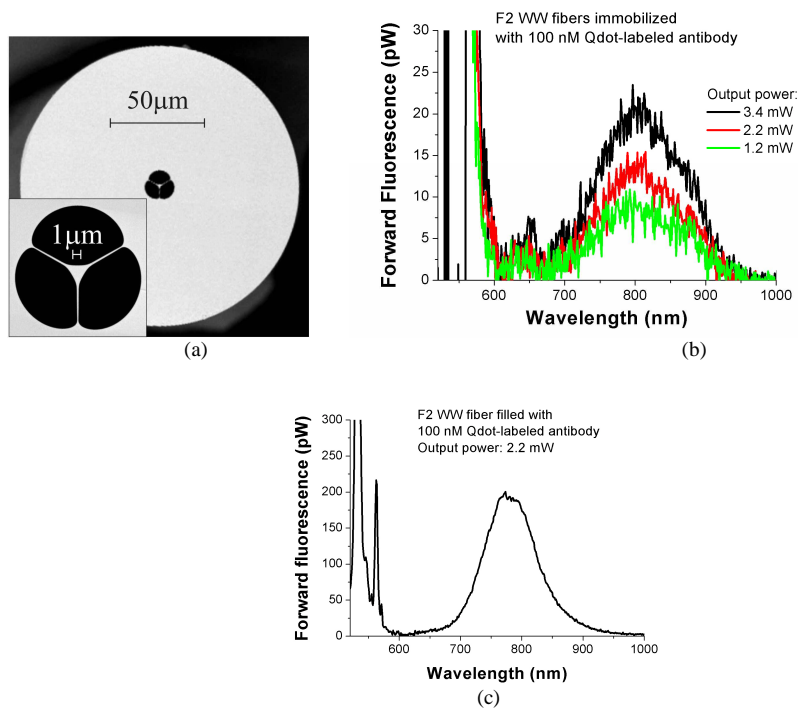


Fig. 4. Fluorescence intensity captured by the forward propagating mode of F2 MOFs using Qdot 800 labeled antibodies for the case of: (a) the SEM image of the MOF used here; (b) immobilized antibodies on the internal surfaces; (c) holes with a 100 nM solution of antibodies.

5. As a comparison, the ratio of the captured fluorescence for an immobilized fiber with a loss of 2 dB/m is also displayed in Fig. 5(b). This corresponds to assuming that no loss is introduced in the immobilization processes. It can be seen from both figures that the fluorescence signal of the immobilized F2 MOF is strongly dependent on the surface density with which the antibody attaches to the surface of the core.

Using this data, the antibody surface density corresponding to the fluorescence capture ratio of 10% (as defined above) as measured in our experiment can be estimated to be  $1.42 \times 10^{-3}$  fmol/mm<sup>2</sup> as illustrated by a grey dot in Fig. 5(a). If no additional loss is introduced to the fiber during the immobilization process, the relative fluorescence signal of fibre with immobilized antibodies could in principal be increased to 36% as shown in Fig. 5(b) (grey dot). Additionally, the lower loss of the immobilized fiber should also enable much longer fiber to be used for further fluorescence enhancement. Figure 5(c) shows length dependence of the fluorescence capture fraction of the low loss immobilized fiber. It can be seen from these results that the fluorescence signal increases with increasing fiber length, with the highest value occurring for a fiber length of approximately 2 m. For longer lengths the fluorescence decreases due to attenuation of the fluorescence signal along the fiber length. For the surface density of  $1.42 \times 10^{-3}$  fmol/mm<sup>2</sup> achieved in our experiments to date, the maximum fluorescence of the immobilized fibers can be enhanced by a factor of 4 using a 2 m length of the MOF (compared with 19.2 cm length used in these experiments).

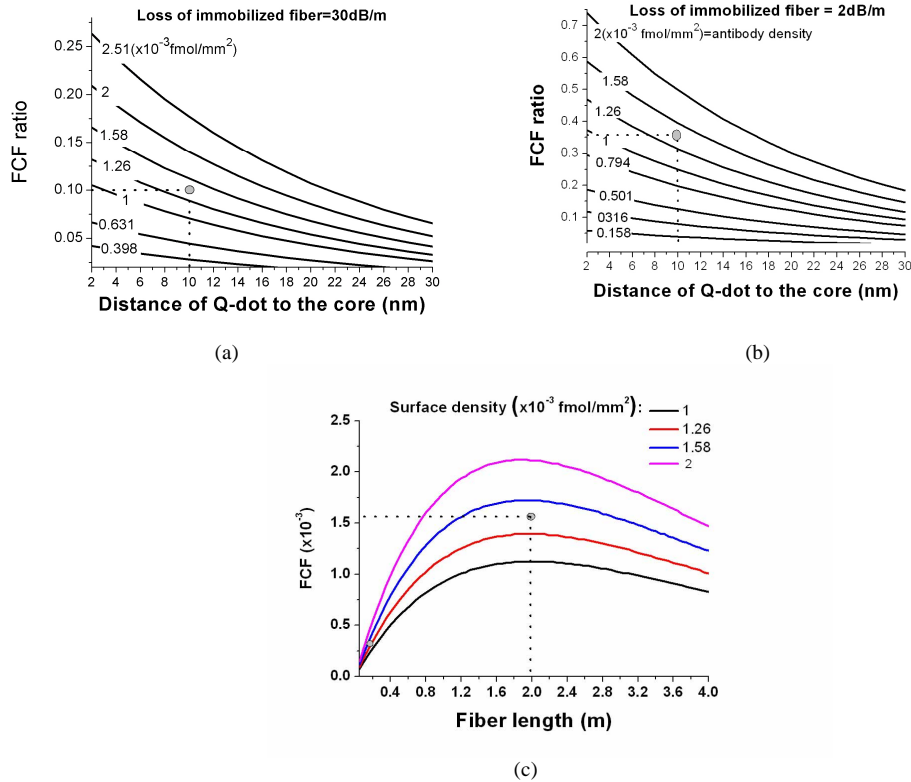


Fig. 5 Comparison of the FCF in the immobilized MOF and in the solution filled MOF. The grey dots in the figures correspond to the points with the surface density of  $1.42 \times 10^{-3} \text{ fmol/mm}^2$ . (a) FCF ratio between two fibers with loss of immobilized fiber of 30 dB/m; (b) FCF ratio with assumed loss of the immobilized fiber as 2 dB/m; (c) length dependence of the FCF with the immobilized fiber loss of 2 dB/m.

Note that the fiber hole radius (approximately  $4 \mu\text{m}$ ) is smaller than the minimum depletion layer thickness of  $9 \mu\text{m}$  measured for a F2 glass plate in Table 1. This suggests that it should be possible to attach all the antibodies within the solution-filled F2 MOF to the internal hole surface, which would amount to an attachment density of  $0.21 \text{ fmol/mm}^2$  based on the size of the F2 MOF used above and the solution concentration of  $100 \text{ nM}$ . This value represents the maximum antibody density that can be immobilized for this fiber. This maximum is 150 times greater than the attached antibody density that we inferred from our experimental results (Fig. 4(a),  $1.42 \times 10^{-3} \text{ fmol/mm}^2$ ). This difference indicates that there is significant scope for substantially improving the magnitude of the fluorescence signal by optimizing the coating processes for improved antibody density.

#### 4. Conclusion

We have successfully demonstrated the adaptation of protein immobilization and binding processes in soft F2 and LLF1 glasses, and achieved good immobilization and binding efficiency. We successfully applied these processes into microstructured fibers made of the F2 glass material. Immobilized proteins have been detected within soft glass MOFs for the first time using fluorescence labeling techniques. This paves the way to sensitive and selective biosensors through binding process. This approach lends itself to the measurement of multiple biomolecules via the immobilization of multiple antibodies. The primary task for building on this work is to optimize the coating procedures to reduce the fiber loss and increase the

density of the attached antibody after processing, which will enable high sensitivity of detection shown by our modeling.

At the same time, the fiber design can be systematically optimized for enhanced fluorescence capture by increasing the mode field fraction in the fiber holes and/or increased field intensity in the glass-air interface [17,20]. Note that when a glass-air interface within a fiber cross-section is located at a point of high intensity within a guided mode, a localized region of high intensity is created on the low-index side, and this effect is particularly striking in high index glasses. Such localized regions can be used to enhance the efficiency of excitation and capture of fluorescent photons for sensing [20]. Thus in the future, improvements in the density of antibodies immobilized on the fiber core surface combined with the deployment of new small-core high-index glass-based MOFs, promises the development of highly sensitive selective biosensors that have ability to compete with existing commercial technologies, such as ELISA [23]. While ELISA is widely used both in research and industry, it lacks the ability to perform real-time in-situ measurements. By adapting this approach to allow the detection of backscattered fluorescence from the input (launch) end of the MOFs, as demonstrated in Ref. [24] for a solution-filled biosensor, this approach promises to lead to the development of biosensors that can move beyond these limitations.

### **Acknowledgments**

We acknowledge funding from DSTO Australia and the Australian Research Council Discovery project DP0665486 for this project, and to S. Afshar and E. Schartner for useful discussions. T. Monro acknowledges the support of an ARC Federation Fellowship.